

ORIGINAL ARTICLE

Plasmin deficiency leads to fibrin accumulation and a compromised inflammatory response in the mouse brain

K. HULTMAN, M. CORTES-CANTELI, A. BOUNOUTAS, A. T. RICHARDS, S. STRICKLAND and E. H. NORRIS

The Rockefeller University, New York, NY, USA

To cite this article: Hultman K, Cortes-Canteli M, Bounoutas A, Richards AT, Strickland S, Norris EH. Plasmin deficiency leads to fibrin accumulation and a compromised inflammatory response in the mouse brain. *J Thromb Haemost* 2014; **12**: 701–12.

Summary. *Background:* Excess fibrin in blood vessels is cleared by plasmin, the key proteolytic enzyme in fibrinolysis. Neurological disorders and head trauma can result in the disruption of the neurovasculature and the entry of fibrin and other blood components into the brain, which may contribute to further neurological dysfunction. *Objectives:* While chronic fibrin deposition is often implicated in neurological disorders, the pathological contributions attributable specifically to fibrin have been difficult to ascertain. An animal model that spontaneously acquires fibrin deposits could allow researchers to better understand the impact of fibrin in neurological disorders. *Methods:* Brains of plasminogen (*plg*)- and tissue plasminogen activator (*tPA*)-deficient mice were examined and characterized with regard to fibrin accumulation, vascular and neuronal health, and inflammation. Furthermore, the inflammatory response following intrahippocampal lipopolysaccharide (LPS) injection was compared between *plg*^{-/-} and wild type (WT) mice. *Results and Conclusions:* Both *plg*^{-/-} and *tPA*^{-/-} mice exhibited brain parenchymal fibrin deposits that appear to result from reduced neurovascular integrity. Markers of neuronal health and inflammation were not significantly affected by proximity to the vascular lesions. A compromised neuroinflammatory response was also observed in *plg*^{-/-} compared to WT mice following intrahippocampal LPS injection. These results demonstrate that fibrin does not affect neuronal health in the absence of inflammation and suggest that plasmin may be necessary for a normal neuroinflammatory response in the mouse CNS.

Correspondence: Erin H. Norris, Laboratory of Neurobiology and Genetics, The Rockefeller University, 1230 York Avenue, Box 169, New York, NY 10065, USA.

Tel.: +1 212 327 8707; fax: +1 212 327 8774.

E-mail: enorris@rockefeller.edu

Received 11 June 2013

Manuscript handled by: R. Medcalf

Final decision: P. H. Reitsma, 19 February 2014

Keywords: fibrin; inflammation; plasmin; tissue plasminogen activator; vasculature.

Introduction

Neurological disorders and head trauma can result in the disruption of the neurovasculature and the entry of blood proteins, such as fibrinogen, into the brain, which may promote deleterious effects when introduced into the brain parenchyma. Fibrinogen is a circulating protein that is required for normal hemostasis. In the event of injury, fibrinogen is cleaved by thrombin to form fibrin, the primary protein component of blood clots. Fibrin is normally excluded from the brain by the blood–brain barrier (BBB). However, following head trauma and chronic neurological disorders such as multiple sclerosis (MS) and Alzheimer's disease (AD), the persistence of fibrin in the brain can potentially worsen and accelerate disease pathology [1]. Both MS and AD patients exhibit increased BBB permeability and fibrin immunostaining in the brain parenchyma [2,3]. In experiments with AD mouse models, fibrin levels correlate with neuroinflammation, BBB disruption, cerebral amyloid angiopathy, and cognitive dysfunction [4,5]. Moreover, depletion of fibrin reduces pathological severity in murine models of MS [6,7] and AD [5].

While chronic fibrin deposition is implicated in the progression of these diseases, the contributions attributable specifically to fibrin are difficult to ascertain. Characterization of its effects requires an animal model that spontaneously acquires brain fibrin deposits in the absence of additional autoimmune or neurodegenerative features. In the WT animal, levels of deposited fibrin are tightly regulated by fibrinolysis, which is driven by the enzyme plasmin. Plasminogen, the precursor of plasmin, binds fibrin and is converted to plasmin by plasminogen activators [8]. Plasmin then degrades fibrin through proteolytic cleavage at specific amino acid residues [8]. Mice deficient in plasminogen (*plg*^{-/-}) are viable but exhibit decreased growth rates and wasting after 3 months [9,10]. The *plg*^{-/-} animals are predisposed to severe thrombosis and

develop spontaneous thrombotic lesions in visceral organs that are associated with fibrin deposition [9,10]. Genetic depletion of fibrin in these animals corrects these phenotypes and restores their normal lifespan [11], suggesting that the widespread deposition of fibrin is toxic. However, chronic fibrin deposition in the brain and its subsequent effects have yet to be investigated.

In the present study, we discovered naturally occurring fibrin deposits in the brains of *plg*^{-/-} mice and investigated the effects of these deposits on vascular, neuronal, and inflammatory markers. Additionally, we compared the inflammatory response to lipopolysaccharide (LPS) in the brains of WT and *plg*^{-/-} mice.

Material and methods

Animals

Plg^{-/-} [9,10], *tPA*^{-/-} [12], and WT littermates or C57/BL6 (Jackson Laboratories, Bar Harbor, ME, USA) mice were used. Genotypes were determined by PCR analysis of tail tissue samples. Both genders of *plg*^{-/-} mice were used in all experiments, and the proportion of females to males was consistent. Mice were maintained in The Rockefeller University's Comparative Biosciences Center and treated in accordance with IACUC-approved protocols.

Stereotactic intrahippocampal injection of LPS

The *plg*^{-/-} and WT control mice ($n = 6-8$ animals per genotype and gender, 12-14 weeks of age) were anesthetized with an intraperitoneal injection of tribromoethanol (0.02 mL g body weight⁻¹) and atropine (0.6 µg g body weight⁻¹) and immobilized in a stereotaxic apparatus. A unilateral intrahippocampal injection of 4 µg µL⁻¹ LPS (1 µL, *Escherichia coli*; Sigma Aldrich, St. Louis, MO, USA) was delivered over a 2-min period. Stereotaxic coordinates from bregma were 2.5 mm posterior, 1.7 mm lateral, and 1.8 mm ventral. Mice were anesthetized 24 h after intrahippocampal LPS injection with an intraperitoneal injection of tribromoethanol and perfused with a solution of 0.9% saline containing heparin. Left and right hippocampi were dissected and stored at -80 °C before RNA or protein extraction, or the whole brain was frozen in Tissue-Tek optimal cutting temperature (OCT) compound (Sakura Finetek, Torrance, CA, USA) before immunohistochemical analysis.

RNA extraction and qPCR

Total RNA was extracted from mouse brain tissue using the Qiagen RNeasy procedure (Qiagen, Valencia, CA, USA), and recovered RNA concentrations were measured using a NanoDrop[®] ND-1000 spectrophotometer (NanoDrop Technologies, Wilmington, DE, USA). RNA was converted to cDNA with a GeneAmp RNA PCR kit

(Applied Biosystems, Foster City, CA, USA). Target mRNA was quantified by quantitative-PCR (qPCR) and normalized relative to ribosomal 18S (r18S) mRNA. The qPCR analysis was performed in a 96-well format on an ABI Prism 7900HT Sequence Detection System (Applied Biosystems). For amplification of target genes, pre-designed primers and probes from Applied Biosystems were used: interleukin-1β (IL-1β) (Mm00434228_m1), tumor necrosis factor-α (TNF-α) (Mm00443260_g1), interleukin-6 (IL-6) (Mm00446190_m1), and r18S (Mm02601777_g1). Relative quantification of gene expression was analyzed as a treatment-to-control expression ratio using the comparative $\Delta\Delta C_t$ method. Each sample was analyzed in triplicate on two separate occasions.

Protein extraction and ELISA

Total protein was extracted from mouse brain tissue using a neuronal protein extraction reagent (Thermo Scientific, Waltham, MA, USA), according to the manufacturer's protocol. Antigen levels of TNF-α, IL-6, and IL-1β were determined by mouse ELISA kits (Abcam, Cambridge, MA, USA), according to the manufacturer's protocol. Each sample was tested in duplicate.

Immunohistochemistry

Plg^{-/-} ($n = 15$ animals including nine females and six males, 2-14 weeks of age used for time course analysis of parenchymal fibrin deposition, and $n = 12$ animals including six females and six males, 12-14 weeks-of age used for all other immunohistological analyses), *tPA*^{-/-} ($n = 4$ animals including three females and one male, 14-16 weeks of age), and WT ($n = 7$ animals including four females and three males, 12-13 weeks of age) mice were perfused with a solution of 0.9% saline containing heparin and their brains were extracted, frozen in OCT compound, and sliced coronally with a cryostat to produce 20 µm-thick sections. Sections were mounted on slides, air dried for 30 min, and fixed in ethanol at -20 °C.

For fibrin and α-smooth muscle actin (α-SMA), glial fibrillary acid protein (GFAP), neutrophils (NIMP-R14), albumin, microtubule-associated protein-2 (MAP-2), CD45, or CD31 co-immunostaining, slides were blocked in 3% goat serum/0.25% Triton X-100 in PBS. For fibrin co-staining with CD11b or ionized calcium binding adaptor molecule-1 (Iba-1), slides were blocked in 3% goat serum in PBS. Primary antibodies were incubated overnight at 4 °C, and secondary fluorescence antibodies were incubated for 1 h at room temperature in the same blocking solution. Also, 4',6-diaminidinium-2-phenylindole (DAPI) was included in the secondary solution to visualize nuclei. For fibrin co-staining with NeuN, the M.O.M. Kit (Vector Laboratories, Burlingame, CA, USA) was used according to the manufacturer's instructions. All slides were then incubated with anti-fibrin(ogen)-FITC

antibody for 2 h at room temperature and subsequently with Sudan Black B solution (Sigma-Aldrich, St. Louis, MO, USA) for 1 min. Vectashield mounting medium (Vector) was used to affix coverslips.

For fibrin and Fluoro-Jade C (FJC; Histo-Chem, Inc., Jefferson, AR, USA) co-staining, slides were blocked in 3% goat serum/0.25% Triton X-100 in PBS and incubated with anti-fibrin(ogen) antibody overnight in the same blocking solution. Subsequently, the sections were incubated for 1 h with Alexa Fluor 555 and DAPI and counterstained for FJC following the manufacturer's instructions. Briefly, sections were immersed in 0.06% KMnO₄ and subsequently in FJC solution (0.00025% FJC in 0.1% acetic acid) for 15 min at room temperature. FJC-stained slides were dried at 50 °C and immersed in clearing agent (Citri-Solv™; Fisher Scientific, Pittsburgh, PA, USA), and coverslips were affixed with Vectamount (Vector).

Collagenase-induced intracerebral hemorrhagic mouse brain tissue sections [13] were used as positive controls for albumin, CD45, and neutrophil immunostainings, whereas brain tissue sections from AD mice [14] were used as positive controls for Iba-1, CD11b, and GFAP immunostaining. Brain sections from mice exposed to an intrahippocampal kainate injection [15] were used as positive control for FJC immunostaining. Replacement of the primary antibodies by PBS served as negative controls for all stainings.

Primary antibodies used in the study are provided in Table 1. The secondary antibodies used: Alexa Fluor 568 goat anti-rat, Alexa Fluor 568 goat anti-chicken, and Alexa Fluor 555 goat anti-rabbit were all purchased from Invitrogen (Grand Island, NY, USA). Streptavidin Texas Red (Vector) was used with the M.O.M. kit.

Microscopy and immunohistological quantification

For all immunohistochemical analyses, coronal whole brain tissue sections ($n = 3-7$ sections per mouse) were examined using a Zeiss Axiovert 200 microscope (Zeiss, Thornwood, NY, USA) with AxioVision v4.8.1.0 software. Quantifications were performed using ImageJ software

Table 1 Primary antibodies used in the present study

Antibody	Species	Antigen	Source
F0111	Rabbit	Fibrin	Dako
ab6666	Goat	Fibrin	Abcam
ab8878	Rat	CD11b	Abcam
550274	Rat	CD31(PECAM-1)	BD Pharmingen/ Fisher
MCA1388	Rat	CD45	Serotec
Z0334	Rabbit	GFAP	Dako
019-19741	Rabbit	Iba-1	Wako
MAB377	Mouse	NeuN	Millipore
C6198	Mouse	α -smooth muscle-Cy3	Sigma Aldrich
AB5622	Rabbit	MAP-2	Chemicon
sc-59338	Rat	Neutrophil (NIMP-R14)	Santa Cruz
ab106582	Chicken	Albumin	Abcam

(NIH, Bethesda, MD, USA). Quantitative image analysis for the LPS-injected mouse sections was performed on three equally spaced sections through the level of the injection site ($AP \pm 1.0$ mm). Identical intensity thresholds were applied to each image set. To determine the degree of fibrin deposition, whole tissue sections that included the cortex, hippocampus, and thalamus were examined, and the total number of fibrin deposits per mouse brain section was determined. Quantification of neuronal and dendritic density was performed on images acquired from non-overlapping cortical areas (that were at least 100 μ m apart) containing or lacking fibrin deposits. Fibrin deposits overlapping with intense CD11b/Iba-1 or GFAP immunostaining were considered positive for reactive microglia and astrocytes, respectively. Micrographs for all figures were taken using a TCS SP8 laser scanning confocal microscope (Leica Microsystems, Wetzlar, Germany). Z-stacks were acquired for Figs 1 and 2, single planes for Figs 3 and 4, and Z-stack tile scan images for Fig. 5.

Statistical analysis

Values are presented as mean \pm SEM, and $P < 0.05$ was considered statistically significant. Linear regression was used to analyze the time course of fibrin deposition (Fig. 1C). Student's *t*-test was used to analyze the effects of fibrin deposition on markers of neuronal health (Fig. 3) and changes in microglial activation (Fig. 5). Changes in mRNA and protein expression of proinflammatory cytokines following intrahippocampal LPS injection (Fig. 6) were evaluated by the linear mixed-effects model. R (R Foundation for Statistical Computing, Vienna, Austria), SPSS (IBM, Armonk, NY, USA), or GraphPad Prism (San Diego, CA, USA) was used for statistical calculations.

Results

Fibrin accumulates in the brains of $plg^{-/-}$ and $tPA^{-/-}$ mice

$Plg^{-/-}$ mice accumulate fibrin in visceral organs including the lung, liver, stomach, gastrointestinal tract, rectum, thymus, and adrenal tissue [9,10]. To determine whether fibrin may also be deposited in the CNS of these mice, brain sections from $plg^{-/-}$ and WT animals were immunostained for fibrin. The $plg^{-/-}$ brains exhibited widespread parenchymal fibrin deposits, which were fibrillar in appearance and ranged from 5 μ m to several hundred microns in diameter (Fig. 1A,B). These deposits did not appear to be region-specific and were found throughout the brain parenchyma (e.g. cortex, hippocampus, and thalamus; olfactory bulbs were not examined). Fibrin deposition was observed in $plg^{-/-}$ animals as young as 2 weeks of age and increased significantly in number (Fig. 1C) and size (data not shown) as the animals matured. Despite evident gender differences observed in

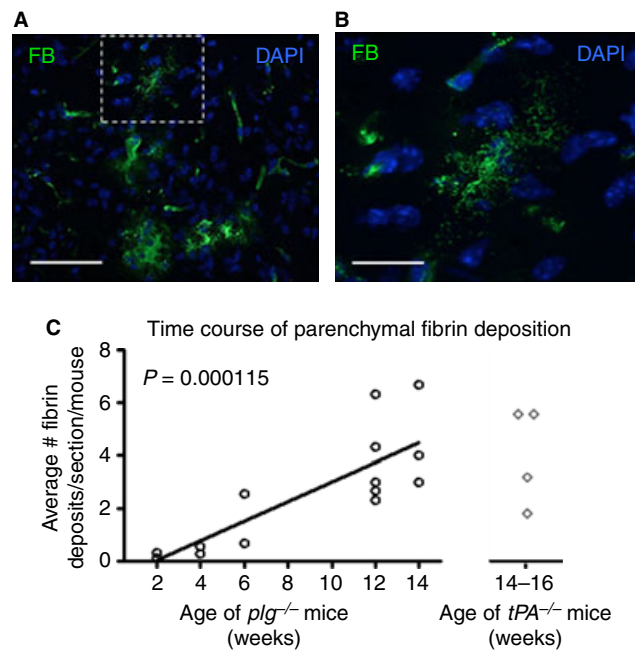


Fig. 1. Mice deficient in *plg* or *tPA* accumulate brain parenchymal fibrin deposits. (A) Anti-fibrin(ogen) antibody reveals representative parenchymal deposits of fibrin (FB, green) in *plg*^{-/-} mouse brains. Scale bar = 60 μ m. (B) Higher magnification of fibrin deposit marked with dashed box in (A). Scale bar = 20 μ m. Maximum projections of confocal Z-stacks are shown. DAPI, blue. (C) Time course of parenchymal fibrin deposition in *plg*^{-/-} mouse brains. Coronal whole brain tissue sections (comprised of the cortex, hippocampus, and thalamus, $n = 3$ –5 sections per animal) were quantified. Each data point represents the average number of deposits per section and animal ($n = 2$ –5 animals per age group). The number of deposits significantly increased over time ($P = 0.000115$; linear regression). The estimated slope suggests an average increase in 0.3715 deposits per week. Mice deficient in *tPA* showed a similar degree of fibrin deposition at 14–16 weeks of age compared to *plg*^{-/-} mice of similar age ($n = 4$ mice, 3–5 sections per animal).

molecular pathways associated with tumor growth in *plg*^{-/-} mice [16], there was no significant difference in the total number of fibrin deposits between female and male *plg*^{-/-} mouse brains. Parenchymal fibrin deposits were also found throughout the brains of *tPA*^{-/-} mice, and there was no significant difference in the number of fibrin deposits between *tPA*^{-/-} and *plg*^{-/-} mice at ~14 weeks of age (Fig. 1C). In contrast, brain parenchymal fibrin deposits were not observed in WT controls.

To identify the source of the fibrin deposits, brain sections from *plg*^{-/-}, *tPA*^{-/-}, and WT mice were co-immunostained for fibrin and CD31/PECAM-1, a marker for vascular endothelial cells [17]. While there was no evidence of extravascular fibrin deposition in WT mice (Fig. 2A), parenchymal fibrin deposits were often observed in direct or close proximity to blood vessels in *plg*^{-/-} (Fig. 2B) and *tPA*^{-/-} (data not shown) mice. Co-staining for α -SMA, a protein present in contractile vessels [18], demonstrated that some fibrin deposits may arise from brain arterioles (Fig. 2C). To further investigate the source of parenchymal fibrin deposits, brain tissue sections were stained for albumin. In both *plg*^{-/-} and *tPA*^{-/-} mice, albumin-positive immunoreactive areas were occasionally observed in the brain parenchyma (data not shown), thus indicating impairment of neurovascular integrity in these mice.

Neuronal health in *plg*^{-/-} and *tPA*^{-/-} mouse brains is not affected by fibrin deposits

In *plg*^{-/-} mice, necrosis is often observed adjacent to thrombotic lesions in the liver and gastrointestinal tract [9]. To determine if brain parenchymal fibrin deposits produce widespread neuronal death, brain sections from *plg*^{-/-}, *tPA*^{-/-}, and WT mice were co-immunostained for fibrin and NeuN, a neuronal nuclei marker [19]. Parenchymal fibrin deposits did not appear to influence neuronal density in *plg*^{-/-} (Fig. 3A,B) or *tPA*^{-/-} mice (data not shown; mean and SEM, 3.27 ± 0.65 in fibrin and 2.9 ± 0.31 in non-fibrin areas, $n = 4$ animals). Moreover, staining of brain sections with FJC, a marker of neuronal degeneration [20], failed to show degenerating neurons around fibrin deposits in *plg*^{-/-} (Fig. 3C) and *tPA*^{-/-} (data not shown) mice. Tissue sections from brains of mice injected intrahippocampally with kainate were used as positive controls for FJC staining (Fig. S1A).

The effects of fibrin deposits on dendritic density were also investigated. Co-staining with antibodies against fibrin and MAP-2, a marker of dendritic density [21], demonstrated co-localization at sites of fibrin deposits without any significant reduction in dendritic marker intensity in *plg*^{-/-} (Fig. 3D,E) and *tPA*^{-/-} mice (data not shown; mean and SEM, 9.89 ± 0.84 in fibrin and

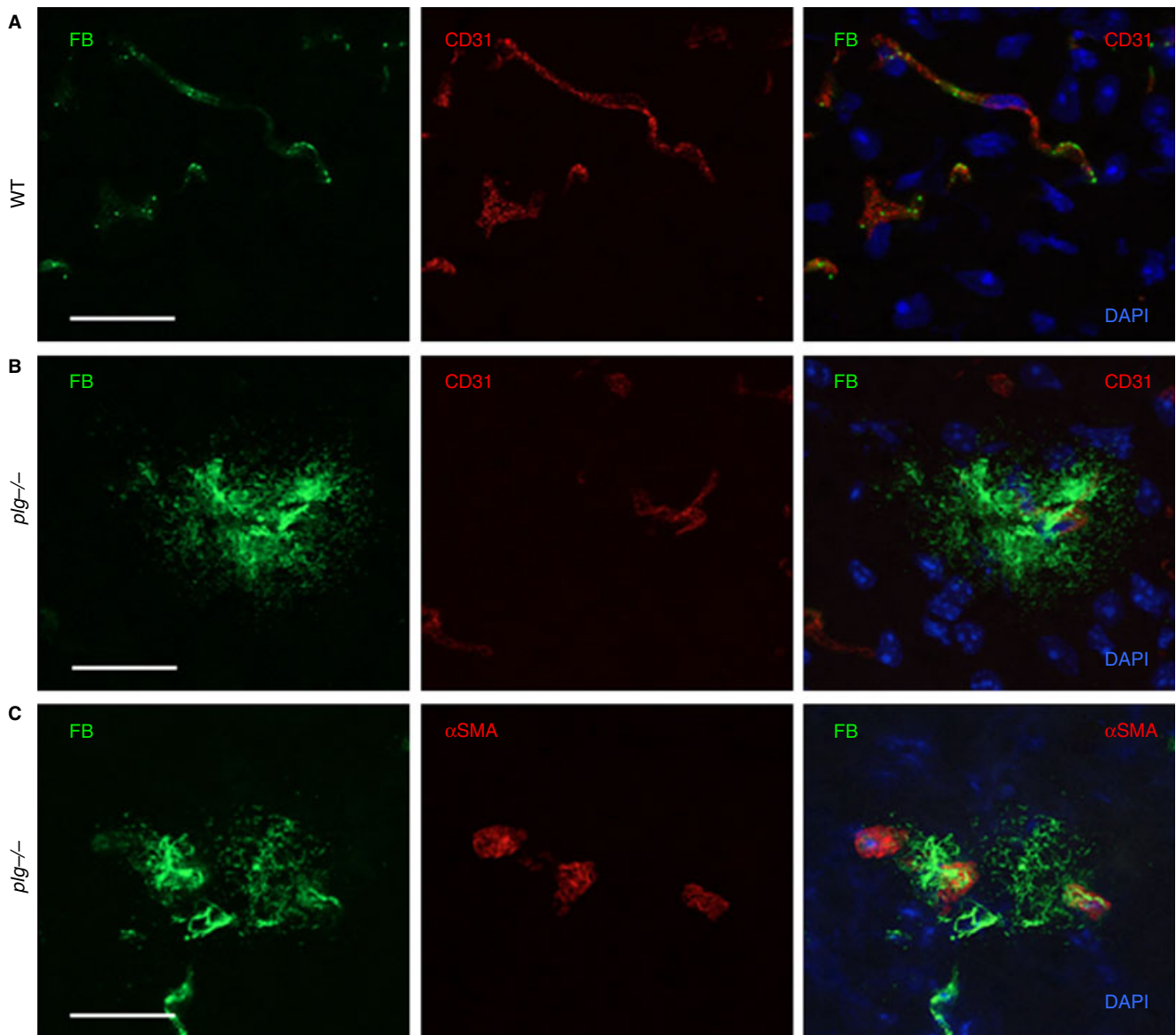


Fig. 2. Fibrin deposits are often located in close proximity to blood vessels in $plg^{-/-}$ brains. Coronal brain sections from $plg^{-/-}$ and WT animals were analyzed by immunohistochemistry. (A) Co-immunostaining against fibrin (FB, green) and CD31 (red) in sections from WT animals did not show any fibrin deposits in the brain parenchyma. (B) Fibrin deposits in $plg^{-/-}$ mice were often observed in close proximity to blood vessels, as demonstrated by co-immunostaining for fibrin (green) and CD31 (red). (C) Fibrin deposits may also arise from brain arterioles in $plg^{-/-}$ mice, as demonstrated by co-immunostaining for fibrin (green) and α -smooth muscle actin (α -SMA, red). Scale bars = 20 μ m. Maximum projections of confocal Z-stacks are shown. DAPI, blue.

11.36 ± 0.90 in non-fibrin areas, $n = 4$ animals). Furthermore, there was no significant difference in neuronal or dendritic density between female and male $plg^{-/-}$ mouse brains (data not shown). Together, these results suggest that gross neuronal and dendritic densities are not affected by the close proximity to fibrin deposits.

Fibrin deposits in $plg^{-/-}$ and $tPA^{-/-}$ mouse brains co-localize with active astrocytes but not microglia

The primary mediators of inflammation in the CNS are microglia and astrocytes, and fibrin can activate both of

these cell types [4,22,23]. Fibrin can also bind the integrin $\alpha_M\beta_2$ receptor CD11b found on monocytes, macrophages, and microglia [22,24], which can result in increased expression of proinflammatory cytokines [25,26]. The inflammatory properties of fibrin deposits in $plg^{-/-}$ and $tPA^{-/-}$ mouse brains were examined by looking for co-localization between deposits and activated microglia or astrocytes. Activated microglia were identified by staining for CD11b [27] and Iba-1 [28]. The vast majority of fibrin deposits in $plg^{-/-}$ mice failed to co-localize with CD11b or Iba-1 immunopositive cells (98.9%, $n = 204$ deposits, and 95.7%, $n = 192$ deposits, respectively) (Fig. 4A,B,E).

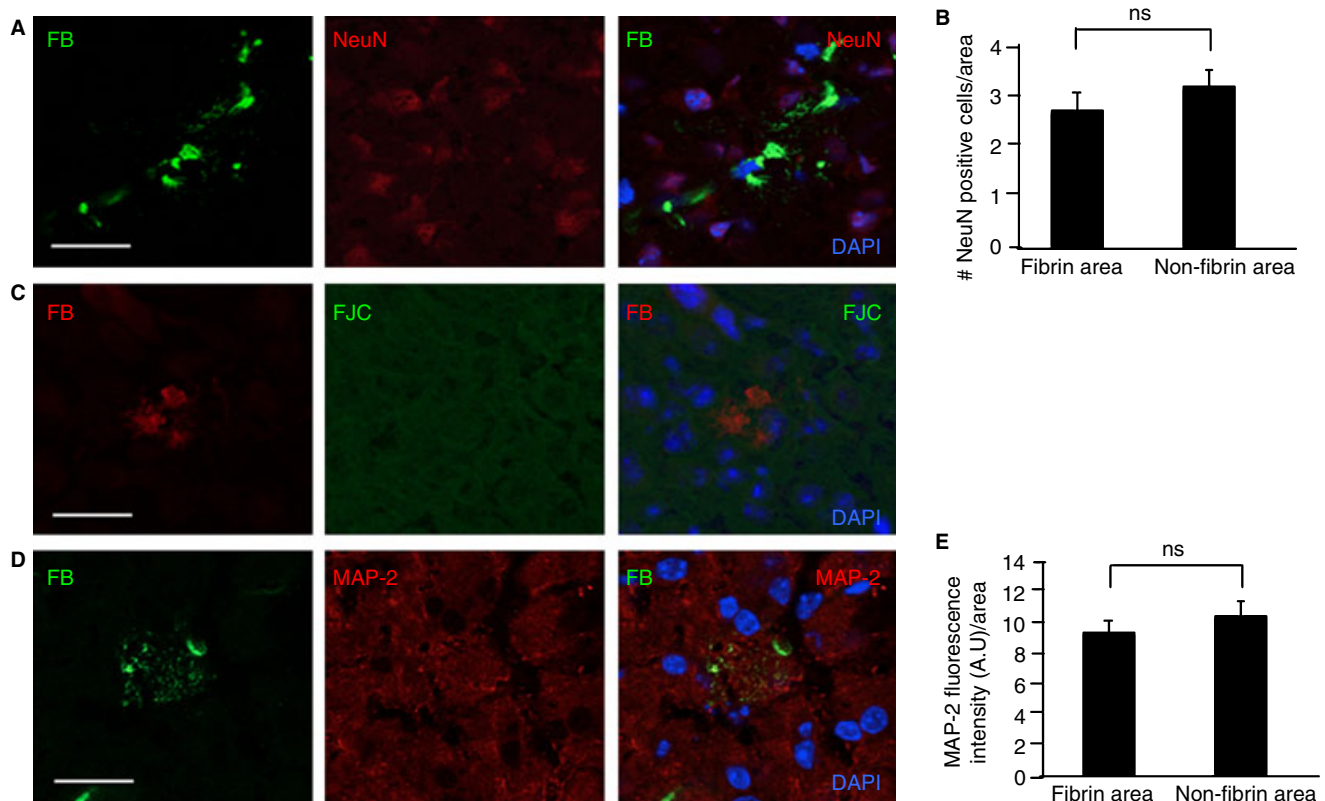


Fig. 3. Fibrin deposits in $plg^{-/-}$ mouse brains do not significantly affect neuronal health. Coronal brain tissue sections from $plg^{-/-}$ animals ($n = 12$ mice, 3–5 sections per animal) were stained, and neuronal markers in cortical areas were quantified. (A) Co-immunostaining for fibrin (FB, green) and neuronal nuclei (NeuN, red) does not show a significant loss of neurons in proximity to fibrin deposits. (B) There is no significant difference in number of NeuN-positive cells in fibrin vs. non-fibrin immunoreactive areas. (C) Fibrin deposition does not correlate with neuronal cell death as visualized by co-immunostaining for fibrin (red) and Fluoro-Jade C (FJC, green). (D) Co-immunostaining for fibrin (green) and microtubule-associated protein-2 (MAP-2, red) indicates that fibrin does not have a significant effect on dendritic density. (E) There is no significant difference in MAP-2 fluorescence intensity in fibrin vs. non-fibrin immunoreactive areas. Differences in neuronal markers (NeuN and MAP-2) between fibrin and non-fibrin immunoreactive areas were evaluated by Student's t -test. Values are presented as mean \pm SEM. Scale bars = 20 μ m. DAPI, blue.

This observation was also true for large fibrin deposits ($\geq 100 \mu$ m), suggesting that the lack of microglial response to the deposits was not a matter of scale. Immunostaining for GFAP, a cytoskeletal marker for active astrocytes [29], demonstrated that more than half of the fibrin deposits (59.5%, $n = 177$ deposits) associated with GFAP-positive cells in $plg^{-/-}$ mouse brains (Fig. 4C,E). No significant difference was observed in degree of co-localization of fibrin with activated microglia or astrocytes between female and male $plg^{-/-}$ mice (data not shown). Immunostaining of $tPA^{-/-}$ mouse brain tissue demonstrated a similar inflammatory response to fibrin deposits in that the vast majority of fibrin deposits failed to co-localize with CD11b (98.3%, $n = 44$ deposits) and Iba-1 (97.3%, $n = 56$ deposits), whereas approximately half of the deposits co-localized with GFAP (52.5%, $n = 32$ deposits). There were no significant differences in microglial or astrocyte activation in areas lacking fibrin deposits among $plg^{-/-}$, $tPA^{-/-}$, and WT mice (data not shown). AD mouse brains were used as positive control

tissue for CD11b, Iba-1, and GFAP immunostaining (Fig. S1B–D).

Fibrin deposits are not associated with neutrophil or macrophage infiltration in $plg^{-/-}$ or $tPA^{-/-}$ mouse brains

Plasmin and plasmin-derived fibrin(ogen) degradation products are potent chemotactic proteins for inflammatory cells, including macrophages and neutrophils [30]. To investigate if fibrin deposition results in recruitment of inflammatory cells, brain sections from $plg^{-/-}$ and $tPA^{-/-}$ mice were co-immunostained for fibrin and CD45, a marker for macrophages/leukocytes [31], and for fibrin and neutrophils. The majority of fibrin deposits failed to co-localize with CD45 (Fig. 4D,E; 97.3%, $n = 71$ deposits) or neutrophils (data not shown; 94.9%, $n = 118$ deposits). No significant difference was observed in the degree of fibrin co-localization with CD45 or neutrophils between female and male $plg^{-/-}$ mice. In $tPA^{-/-}$ animals, 94.1% and 95.0% of the fibrin deposits

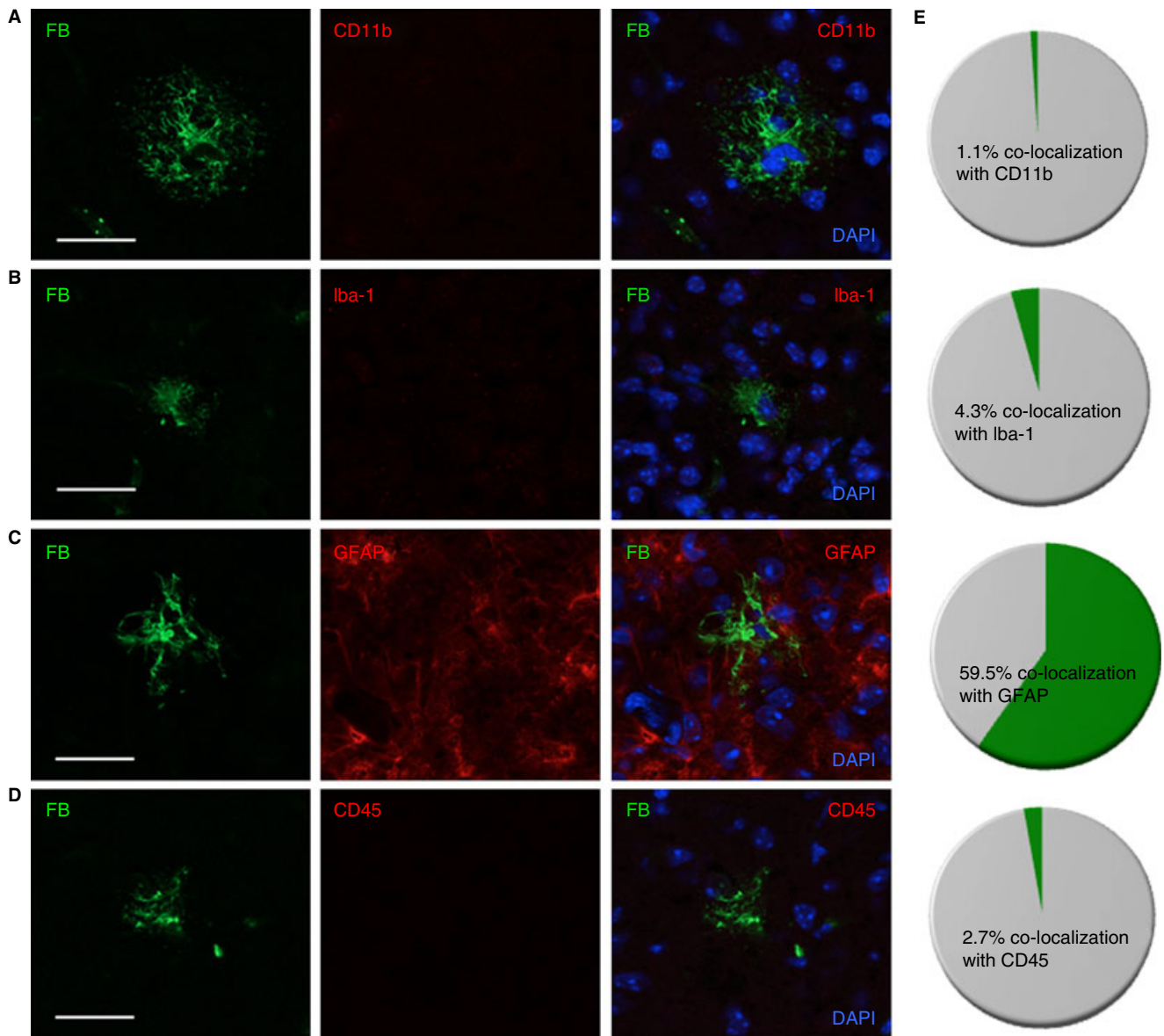


Fig. 4. Fibrin deposits in $plg^{-/-}$ mouse brains co-localize with reactive astrocytes but not microglia or lymphocytes/macrophages. Coronal brain tissue sections from $plg^{-/-}$ mice ($n = 12$ mice, 3–5 sections per animal) were stained and quantified. Co-immunostaining for (A) fibrin (FB, green) and CD11b (red) or (B) fibrin (green) and Iba-1 (red) showed that fibrin deposits do not co-localize with activated microglia. (C) Fibrin deposits co-localize with activated astrocytes, as demonstrated by co-immunostaining for fibrin (green) and GFAP (red). (D) Co-immunostaining for fibrin (green) and CD45 (red) shows that fibrin deposits do not co-localize with lymphocytes/macrophages. Scale bars = 20 μ m. (E) Pie graphs show the percentage of fibrin deposits that co-localize with CD11b, Iba-1, GFAP, and CD45 staining ($n = 204$ deposits for FB-CD11b co-localization; $n = 192$ deposits for FB-Iba-1 co-localization; $n = 177$ deposits for FB-GFAP co-localization, and $n = 71$ for FB-CD45 co-localization).

($n = 24$ – 29 deposits) failed to co-localize with CD45 and neutrophils, respectively (data not shown). Brain tissue sections from mice with intracerebral hemorrhage were used as positive controls for CD45 staining (Fig. S1E).

Reduced neuroinflammatory response to LPS in $plg^{-/-}$ mice

Because fibrin deposits in $plg^{-/-}$ mouse brains did not provoke a significant activation of microglia, we hypothe-

sized that these animals may have a compromised inflammatory response in the CNS. To test this idea, the response to LPS, a common inflammagen used to activate microglia and provoke induction of proinflammatory cytokine expression *in vivo* [32], was compared between $plg^{-/-}$ and WT mouse brains. Animals received a unilateral intrahippocampal injection of LPS, and the activation of microglia and astrocytes as well as the expression of proinflammatory cytokines were analyzed 24 h later. Immuno-

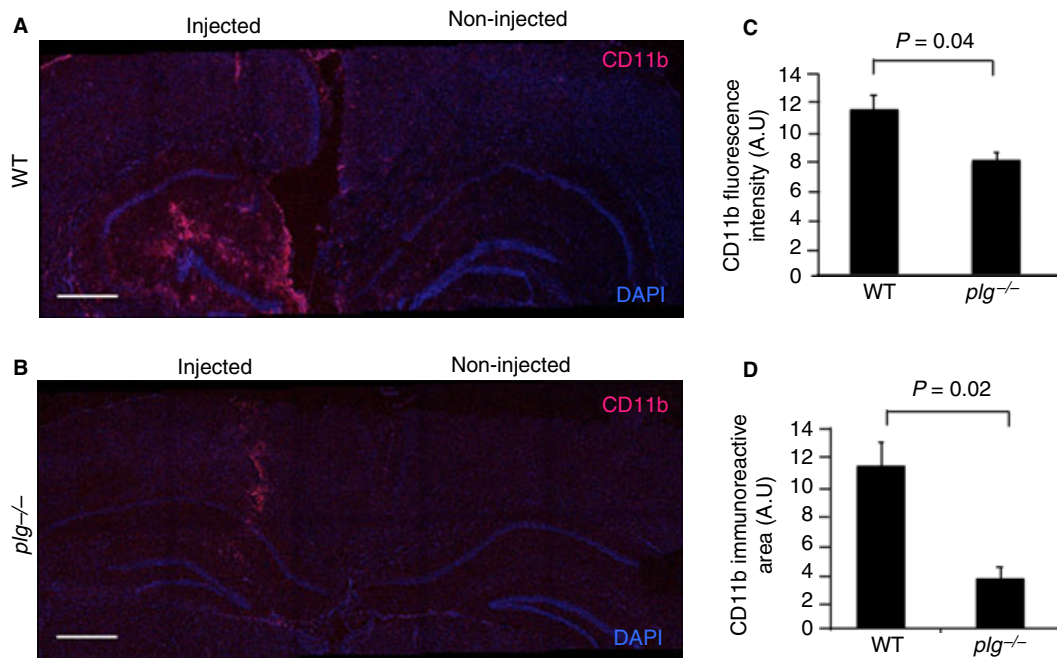


Fig. 5. Reduced microglial activation in response to LPS in *plg*^{-/-} mouse brains. WT ($n = 2$) and *plg*^{-/-} ($n = 4$) mice received a unilateral intrahippocampal injection of LPS. Brains were collected 24 h post-injection and immunostained for activated microglia (CD11b). Maximum projections of confocal Z-stack tile-scans covering the cortex and hippocampus of injected and non-injected hemispheres are shown for CD11b (red) staining and DAPI (blue) from a (A) WT and (B) *plg*^{-/-} mouse. Scale bars=20 μ m. Quantification of microglial activation indicated significantly reduced (C) CD11b fluorescence intensity and (D) CD11b immunoreactive area in LPS-injected hippocampi of *plg*^{-/-} compared to WT mice. Differences in fluorescence intensity and immunoreactive area between the genotypes were evaluated by Student's *t*-test. Values are presented as mean \pm SEM.

histochemical analysis using anti-CD11b antibody revealed that activation of microglia was markedly reduced in the LPS-injected hemispheres of *plg*^{-/-} compared to WT mice (Fig. 5A vs. B) as both CD11b fluorescence intensity (Fig. 5C) and CD11b immunoreactive area (Fig. 5D) were significantly lower in *plg*^{-/-} compared to controls. In contrast, there was no significant difference in astrocyte activation, measured by fluorescence intensity and immunoreactive area of GFAP, between LPS-injected hemispheres of *plg*^{-/-} and WT mice (data not shown). Furthermore, a pronounced difference in the induction of pro-inflammatory cytokine expression was observed between the two genotypes. As expected [32], intrahippocampal LPS injection resulted in a marked up-regulation of TNF- α , IL-1 β , and IL-6 mRNA (Fig. 6A,C,E) and protein expression (Fig. 6B,D,F) levels compared to the contralateral non-injected hippocampus. On the contrary, up-regulation of these proinflammatory cytokines was significantly reduced in the LPS-injected *plg*^{-/-} mouse hippocampus compared to the LPS-injected WT mouse hippocampus (Fig. 6). Moreover, there was no significant up-regulation of proinflammatory cytokine protein levels after LPS injection in the *plg*^{-/-} mouse hippocampus compared to the contralateral non-injected hippocampus (Fig. 6B,D,F). No significant differences in expression levels of these cytokines were observed between non-injected WT and *plg*^{-/-} mouse brains. Together, these results suggest that plasmin is

required for a complete inflammatory response in the mouse brain.

Discussion

Mice deficient in plasminogen have been extensively used for unraveling the role of plasmin(ogen) and its substrate fibrin in physiological and pathophysiological processes. However, the endogenous accumulation of fibrin and its biological effects in the brains of these mice have not been previously investigated. The studies discussed here show that *plg*^{-/-} mice accumulate brain parenchymal fibrin deposits early in life (Fig. 1) that appear to result from reduced neurovascular integrity (Fig. 2), yet these deposits do not impact neuronal health (Fig. 3) or induce local inflammation (Fig. 4). Furthermore, these studies also show that the neuroinflammatory response is impaired in *plg*^{-/-} mice when challenged with a more general inflammatory mediator (Figs 5 and 6). Mice deficient in tPA also exhibit accumulation of fibrin in their brain parenchyma (Fig. 1) without showing any significant inflammatory response to these deposits, thus implying that plasmin, rather than plasminogen, is ultimately required for a complete inflammatory response to fibrin in the CNS.

Fibrin deposits in close proximity to blood vessels and the abundant albumin immunoreactivity in the *plg*^{-/-}

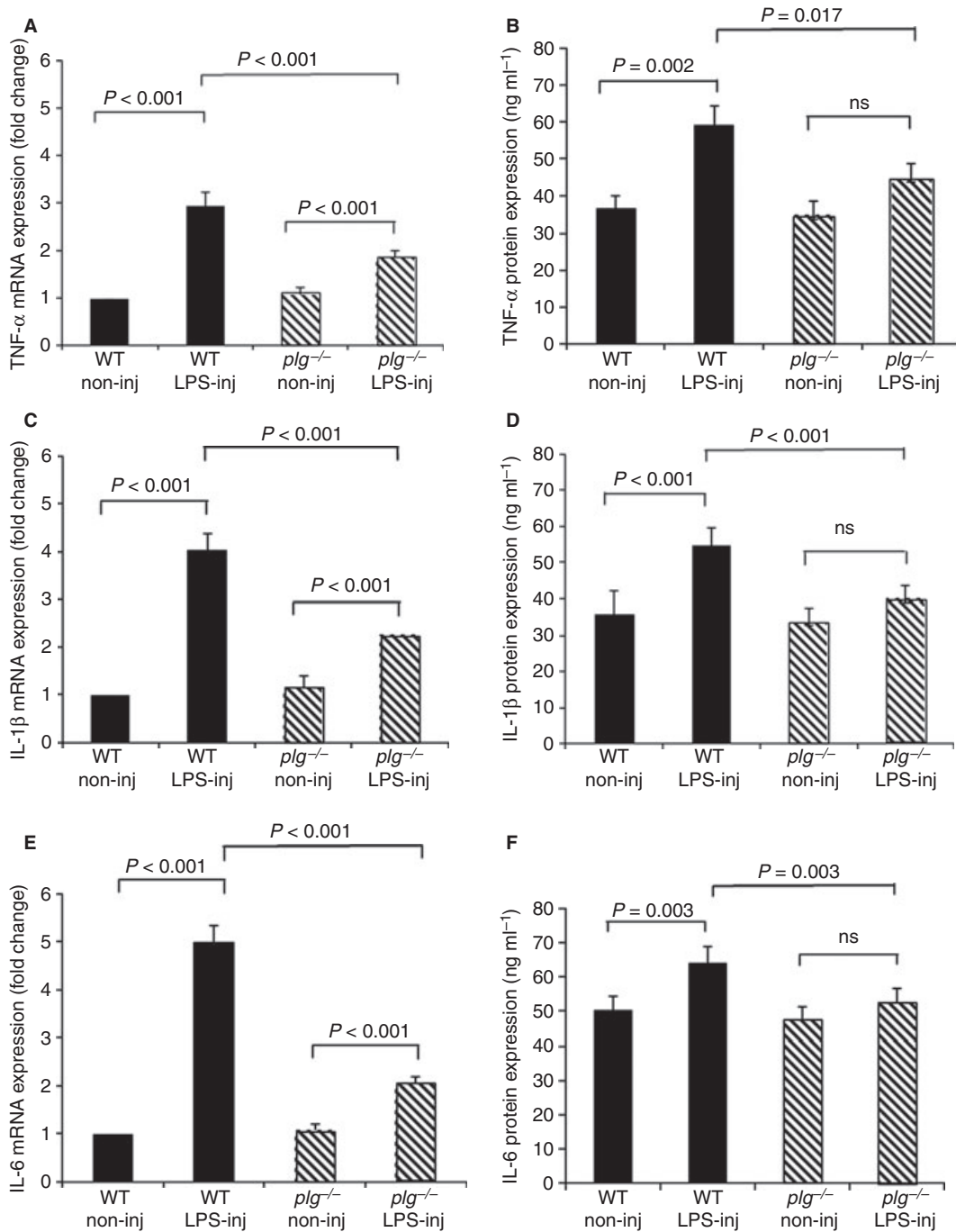


Fig. 6. Reduced induction of proinflammatory cytokine expression in response to LPS in *plg*^{-/-} mouse brains. The *plg*^{-/-} and WT mice ($n = 4$ animals per genotype) received a unilateral intrahippocampal injection of LPS. Injected (LPS-inj) and non-injected (non-inj) hippocampi were collected 24 h post-injection, and expression levels of the proinflammatory cytokines TNF- α (A, mRNA; B, protein), IL-1 β (C, mRNA; D, protein), and IL-6 (E, mRNA; F, protein) were analyzed by qPCR and ELISA. mRNA results are expressed as fold change compared to non-injected WT hippocampus. Results were evaluated by the linear mixed effect model. Values are presented as mean \pm SEM.

mouse brain parenchyma (Fig. 2 and data not shown, respectively) are supported by a previous study showing impairments of neurovascular integrity in *plg*^{-/-} mice at 3 months of age [4]. Similarly, we identified fibrin deposits and altered BBB properties in *tPA*^{-/-} mice (data not shown). Although it is unclear as to how plasmin(ogen) and tPA impact neurovascular integrity, studies indicate

that changes in BBB permeability during pathophysiological conditions may occur via tPA's interaction with lipoprotein receptor-related protein and subsequent activation of matrix metalloproteinases and/or platelet-derived growth factor-CC, which can be associated with detachment of astrocytic endfeet from the basal lamina (reviewed in Ref. [33]). Others have reported studies showing that

fibrin(ogen) decreases expression levels of tight junction proteins *in vitro* [34,35]. Thus, it is possible that our observations in the *plg*^{-/-} and *tPA*^{-/-} mice result from a direct effect of fibrin on cerebrovascular endothelial cells rather than an effect of tPA activity on BBB permeability. We hypothesize that this compromised neurovasculature, together with widespread fibrin deposition, might lead to deficits in cerebral blood flow in these mice. Since hypoperfusion can lead to cognitive decline [36,37], our current findings support our previous report that *plg*^{-/-} mice exhibit memory deficits [5]. Our results also correlate well with what is observed in chronic neurodegenerative diseases in humans, such as MS and AD. Studies on postmortem tissue from these patients often show reduced neurovascular integrity and leakage of fibrin into the brain parenchyma [1–3]. AD and MS patients also present with hypoperfusion [37,38], which could ultimately lead to their cognitive deficits. Future studies that examine the role of plasmin in neurodegenerative disease pathophysiology may be warranted as plasmin may have a significant impact on neurovascular integrity.

Since the extravasation of fibrin into the nervous system can induce local inflammation and may contribute to neurological dysfunction [3–6], we anticipated that these chronic fibrin deposits in *plg*^{-/-} mouse brains would trigger the inflammatory response and subsequently impact neuronal health. Intriguingly, our investigation did not reveal any substantial effect of fibrin deposits on inflammatory/neuronal markers or vascular recruitment of inflammatory cells. This lack of neuroinflammatory response to fibrin prompted us to perform additional *in vivo* experiments to determine whether this response was fibrin specific or more general. The *plg*^{-/-} and WT mice were exposed to the endotoxin LPS via an intrahippocampal injection, and the local inflammatory response was analyzed. These experiments showed that activation of microglial cells and induction of proinflammatory cytokines were significantly reduced in *plg*^{-/-} animals following LPS challenge compared to WT mice. Our findings agree with reports showing significantly reduced activation of immune cells and reduced induction of proinflammatory cytokine expression in response to inflammatory stimuli in peripheral tissues of *plg*^{-/-} mice [39–41]. Supporting our result that fibrin deposition does not induce neuronal death in the absence of neuroinflammation is the report by Davalos *et al.* [42], which showed that mutant mice expressing fibrinogen γ 390-396, which is unable to interact with microglial receptors and induce an inflammatory response, are protected from neuronal damage. Also in line with our results is the study by Schachtrup *et al.* [43], which showed that fibrinogen can affect astrocytes independently of microglial activation. Thus, our combined data suggest that plasmin (ogen) is necessary for a complete inflammatory response peripherally as well as centrally.

Various mechanisms may explain the impaired neuroinflammatory response in *plg*^{-/-} mice. It has been well

established that plasmin and its degradation products are potent activators of inflammatory cells [44–46]. Plasmin also plays an important role in cell migration by facilitating degradation of matrix proteins and activating matrix metalloproteases [47], which is supported by the present finding that fibrin deposits in *plg*^{-/-} mice are not associated with the recruitment of macrophages and neutrophils. Therefore, the impaired inflammatory response in the brains of *plg*^{-/-} mice may result from a lack of plasmin-dependent recruitment and activation of inflammatory cells at sites of fibrin deposition or inflammation. This notion is supported by previous studies in *plg*^{-/-} mice, demonstrating that cell migration associated with the inflammatory response is compromised in peripheral organs of these mice. For example, *plg*^{-/-} mice show diminished migration of smooth muscle cells during wound healing [48], as well as reduced recruitment of macrophages and neutrophils in response to inflammatory mediators [49] and biomaterials [50]. Detailed studies to elucidate the specific roles of plasmin in the neuroinflammatory response are warranted. However, given the blunted inflammatory process in *plg*^{-/-} mice, caution should be taken when utilizing this animal model in studies involving neurological disorders and neuroinflammation.

Based on the results presented in this study, we show that fibrin does not affect neuronal health in the absence of inflammation and that plasmin plays an essential role in maintaining a normal proinflammatory capability in the CNS.

Addendum

K. Hultman is responsible for the concept and design, analysis and interpretation of data, and critical writing of manuscript. M. Cortes-Canteli is responsible for the concept and design and the analysis and interpretation of data. A. Bounoutas is responsible for the concept and design, analysis and interpretation of data, and critical writing of manuscript. A. T. Richards is responsible for the analysis and interpretation of data. S. Strickland is responsible for the concept and design and the revision of intellectual content. E. H. Norris is responsible for the concept and design, interpretation of data, critical writing of manuscript, and revision of intellectual content.

Acknowledgements

This work was supported by National Institutes of Health grant NS50537, Litwin Foundation, May and Samuel Rudin Family Foundation, Blanchette Hooker Rockefeller Fund, John A. Herrmann, Jr., and the Mellam Family Foundation. K.H. was supported by the Swedish Research Council and the Sweden-America Foundation, and A.B. was supported by the American Heart Association. We gratefully thank Dr. Z.-L. Chen for providing positive control and *tPA*^{-/-} mouse brain tissue and all

other members of the Strickland Laboratory for helpful discussions regarding this study. We also thank Dr. Joel Correa da Rosa, biostatistician at The Rockefeller University, for his assistance with statistical analysis.

Disclosure of Conflict of Interest

The authors state that they have no conflicts of interests.

Supporting Information

Additional Supporting Information may be found in the online version of this article:

Fig. S1. Immunostaining of positive control mouse brain tissue specimens. Representative images for (A) Fluoro-Jade C (FJC, green), (B) CD11b (red), (C) Iba-1 (red), (D) GFAP (red), and (E) CD45 (red). Immunostaining for FJC was performed on brain tissue from kainate-injected mice, for CD45 on brain tissue from mice with intracerebral hemorrhage, and for CD11b, Iba-1, and GFAP on brain tissue from AD mice. Scale bars = 20 μ m. DAPI, blue.

References

- Adams RA, Passino M, Sachs BD, Nuriel T, Akassoglou K. Fibrin mechanisms and functions in nervous system pathology. *Mol Interv* 2004; **4**: 163–76.
- Claudio L, Raine CS, Brosnan CF. Evidence of persistent blood-brain barrier abnormalities in chronic-progressive multiple sclerosis. *Acta Neuropathol* 1995; **90**: 228–38.
- Ryu JK, McLarnon JG. A leaky blood-brain barrier, fibrinogen infiltration and microglial reactivity in inflamed Alzheimer's disease brain. *J Cell Mol Med* 2009; **13**: 2911–25.
- Paul J, Strickland S, Melchor JP. Fibrin deposition accelerates neurovascular damage and neuroinflammation in mouse models of Alzheimer's disease. *J Exp Med* 2007; **204**: 1999–2008.
- Cortes-Canteli M, Paul J, Norris EH, Bronstein R, Ahn HJ, Zamolodchikov D, Bhuvanendran S, Fenz KM, Strickland S. Fibrinogen and beta-amyloid association alters thrombosis and fibrinolysis: a possible contributing factor to Alzheimer's disease. *Neuron* 2010; **66**: 695–709.
- Akassoglou K, Adams RA, Bauer J, Mercado P, Tseveleki V, Lassmann H, Probert L, Strickland S. Fibrin depletion decreases inflammation and delays the onset of demyelination in a tumor necrosis factor transgenic mouse model for multiple sclerosis. *Proc Natl Acad Sci U S A* 2004; **101**: 6698–703.
- Inoue A, Koh CS, Shimada K, Yanagisawa N, Yoshimura K. Suppression of cell-transferred experimental autoimmune encephalomyelitis in defibrinated Lewis rats. *J Neuroimmunol* 1996; **71**: 131–7.
- Mosesson MW. Fibrinogen and fibrin structure and functions. *J Thromb Haemost* 2005; **3**: 1894–904.
- Bugge TH, Flick MJ, Daugherty CC, Degen JL. Plasminogen deficiency causes severe thrombosis but is compatible with development and reproduction. *Genes Dev* 1995; **9**: 794–807.
- Ploplis VA, Carmeliet P, Vazirzadeh S, van Vlaenderen I, Moons L, Plow EF, Collen D. Effects of disruption of the plasminogen gene on thrombosis, growth, and health in mice. *Circulation* 1995; **92**: 2585–93.
- Bugge TH, Kombrinck KW, Flick MJ, Daugherty CC, Danton MJ, Degen JL. Loss of fibrinogen rescues mice from the pleiotropic effects of plasminogen deficiency. *Cell* 1996; **87**: 709–19.
- Carmeliet P, Schoonjans L, Kieckens L, Ream B, Degen J, Bronson R, De Vos R, van den Oord JJ, Collen D, Mulligan RC. Physiological consequences of loss of plasminogen activator gene function in mice. *Nature* 1994; **368**: 419–24.
- Tang J, Liu J, Zhou C, Alexander JS, Nanda A, Granger DN, Zhang JH. Mmp-9 deficiency enhances collagenase-induced intracerebral hemorrhage and brain injury in mutant mice. *J Cereb Blood Flow Metab* 2004; **24**: 1133–45.
- Oakley H, Cole SL, Logan S, Maus E, Shao P, Craft J, Guillozet-Bongaarts A, Ohno M, Disterhoft J, van Eldik L, Berry R, Vassar R. Intraneuronal beta-amyloid aggregates, neurodegeneration, and neuron loss in transgenic mice with five familial Alzheimer's disease mutations: potential factors in amyloid plaque formation. *J Neurosci* 2006; **26**: 10129–40.
- Chen ZL, Yu H, Yu WM, Pawlak R, Strickland S. Proteolytic fragments of laminin promote excitotoxic neurodegeneration by up-regulation of the KA1 subunit of the kainate receptor. *J Cell Biol* 2008; **183**: 1299–313.
- Hald A, Eickhardt H, Maerkedahl RB, Feldborg CW, Egerod KL, Engelholm LH, Laerum OD, Lund LR, Rono B. Plasmin-driven fibrinolysis facilitates skin tumor growth in a gender-dependent manner. *FASEB J* 2012; **26**: 4445–57.
- van Mourik JA, Leeksa OC, Reinders JH, de Groot PG, Zandbergen-Spaargaren J. Vascular endothelial cells synthesize a plasma membrane protein indistinguishable from the platelet membrane glycoprotein IIa. *J Biol Chem* 1985; **260**: 11300–6.
- Skalli O, Pelte MF, Pecelet MC, Gabbiani G, Gugliotta P, Bussoleti G, Ravazzola M, Orci L. Alpha-smooth muscle actin, a differentiation marker of smooth muscle cells, is present in microfilamentous bundles of pericytes. *J Histochem Cytochem* 1989; **37**: 315–21.
- Mullen RJ, Buck CR, Smith AM. NeuN, a neuronal specific nuclear protein in vertebrates. *Development* 1992; **116**: 201–11.
- Schmued LC, Albertson C, Slikker W Jr. Fluoro-Jade: a novel fluorochrome for the sensitive and reliable histochemical localization of neuronal degeneration. *Brain Res* 1997; **751**: 37–46.
- Caceres A, Busciglio J, Ferreira A, Steward O. An immunocytochemical and biochemical study of the microtubule-associated protein MAP-2 during post-lesion dendritic remodeling in the central nervous system of adult rats. *Brain Res* 1988; **427**: 233–46.
- Adams RA, Bauer J, Flick MJ, Sikorski SL, Nuriel T, Lassmann H, Degen JL, Akassoglou K. The fibrin-derived γ 377-395 peptide inhibits microglia activation and suppresses relapsing paralysis in central nervous system autoimmune disease. *J Exp Med* 2007; **204**: 571–82.
- Davalos D, Akassoglou K. Fibrinogen as a key regulator of inflammation in disease. *Semin Immunopathol* 2012; **34**: 43–62.
- Ugarova TP, Yakubenko VP. Recognition of fibrinogen by leukocyte integrins. *Ann N Y Acad Sci* 2001; **936**: 368–85.
- Fan ST, Edgington TS. Integrin regulation of leukocyte inflammatory functions. CD11b/CD18 enhancement of the tumor necrosis factor-alpha responses of monocytes. *J Immunol* 1993; **150**: 2972–80.
- Perez RL, Ritzenthaler JD, Roman J. Transcriptional regulation of the interleukin-1beta promoter via fibrinogen engagement of the CD18 integrin receptor. *Am J Respir Cell Mol Biol* 1999; **20**: 1059–66.
- Ling EA, Wong WC. The origin and nature of ramified and amoeboid microglia: a historical review and current concepts. *Glia* 1993; **7**: 9–18.
- Ito D, Imai Y, Ohsawa K, Nakajima K, Fukuuchi Y, Kohsaka S. Microglia-specific localisation of a novel calcium binding protein, Iba1. *Brain Res Mol Brain Res* 1998; **57**: 1–9.
- Ridet JL, Malhotra SK, Privat A, Gage FH. Reactive astrocytes: cellular and molecular cues to biological function. *Trends Neurosci* 1997; **20**: 570–7.

- 30 Syrovets T, Lunov O, Simmet T. Plasmin as a proinflammatory cell activator. *J Leukoc Biol* 2012; **92**: 509–19.
- 31 Zattoni M, Mura ML, Deprez F, Schwendener RA, Engelhardt B, Frei K, Fritschy JM. Brain infiltration of leukocytes contributes to the pathophysiology of temporal lobe epilepsy. *J Neurosci* 2011; **31**: 4037–50.
- 32 Herber DL, Maloney JL, Roth LM, Freeman MJ, Morgan D, Gordon MN. Diverse microglial responses after intrahippocampal administration of lipopolysaccharide. *Glia* 2006; **53**: 382–91.
- 33 Vivien D, Gauberti M, Montagne A, Defer G, Touze E. Impact of tissue plasminogen activator on the neurovascular unit: from clinical data to experimental evidence. *J Cereb Blood Flow Metab* 2011; **31**: 2119–34.
- 34 Tyagi N, Roberts AM, Dean WL, Tyagi SC, Lominadze D. Fibrinogen induces endothelial cell permeability. *Mol Cell Biochem* 2008; **307**: 13–22.
- 35 Patibandla PK, Tyagi N, Dean WL, Tyagi SC, Roberts AM, Lominadze D. Fibrinogen induces alterations of endothelial cell tight junction proteins. *J Cell Physiol* 2009; **221**: 195–203.
- 36 de la Torre JC. Cardiovascular risk factors promote brain hypoperfusion leading to cognitive decline and dementia. *Cardiovasc Psychiatry Neurol* 2012; **2012**: 1–15.
- 37 Staffen W, Bergmann J, Schonauer U, Zauner H, Kronbichler M, Golaszewski S, Ladurner G. Cerebral perfusion (HMPAO-SPECT) in patients with depression with cognitive impairment versus those with mild cognitive impairment and dementia of Alzheimer's type: a semiquantitative and automated evaluation. *Eur J Nucl Med Mol Imaging* 2009; **36**: 801–10.
- 38 D'Haeseleer M, Cambron M, Vanopdenbosch L, De Keyser J. Vascular aspects of multiple sclerosis. *Lancet Neurol* 2011; **10**: 657–66.
- 39 Guo Y, Li J, Hagstrom E, Ny T. Protective effects of plasmin (ogen) in a mouse model of *Staphylococcus aureus*-induced arthritis. *Arthritis Rheum* 2008; **58**: 764–72.
- 40 Guo Y, Li J, Hagstrom E, Ny T. Beneficial and detrimental effects of plasmin(ogen) during infection and sepsis in mice. *PLoS One* 2011; **6**: e24774.
- 41 Li J, Ny A, Leonardsson G, Nandakumar KS, Holmdahl R, Ny T. The plasminogen activator/plasmin system is essential for development of the joint inflammatory phase of collagen type II-induced arthritis. *Am J Pathol* 2005; **166**: 783–92.
- 42 Davalos D, Ryu JK, Merlini M, Baeten KM, Le Moan N, Petersen MA, Deerinck TJ, Smirnoff DS, Bedard C, Hakozi H, Gonias Murray S, Ling JB, Lassmann H, Degen JL, Ellisman MH, Akassoglou K. Fibrinogen-induced perivascular microglial clustering is required for the development of axonal damage in neuroinflammation. *Nat Commun* 2012; **3**: 1227.
- 43 Schachtrup C, Ryu JK, Helmrick MJ, Vagena E, Galanakis DK, Degen JL, Margolis RU, Akassoglou K. Fibrinogen triggers astrocyte scar formation by promoting the availability of active TGF-beta after vascular damage. *J Neurosci* 2010; **30**: 5843–54.
- 44 Syrovets T, Tippler B, Rieks M, Simmet T. Plasmin is a potent and specific chemoattractant for human peripheral monocytes acting via a cyclic guanosine monophosphate-dependent pathway. *Blood* 1997; **89**: 4574–83.
- 45 Syrovets T, Jendrach M, Rohwedder A, Schule A, Simmet T. Plasmin-induced expression of cytokines and tissue factor in human monocytes involves AP-1 and IKKbeta-mediated NF-kappaB activation. *Blood* 2001; **97**: 3941–50.
- 46 Li Q, Laumonier Y, Syrovets T, Simmet T. Plasmin triggers cytokine induction in human monocyte-derived macrophages. *Arterioscler Thromb Vasc Biol* 2007; **27**: 1383–9.
- 47 Rifkin DB. Plasminogen activator expression and matrix degradation. *Matrix Suppl* 1992; **1**: 20–2.
- 48 Carmeliet P, Moons L, Ploplis V, Plow E, Collen D. Impaired arterial neointima formation in mice with disruption of the plasminogen gene. *J Clin Invest* 1997; **99**: 200–8.
- 49 Ploplis VA, French EL, Carmeliet P, Collen D, Plow EF. Plasminogen deficiency differentially affects recruitment of inflammatory cell populations in mice. *Blood* 1998; **91**: 2005–9.
- 50 Busuttill SJ, Ploplis VA, Castellino FJ, Tang L, Eaton JW, Plow EF. A central role for plasminogen in the inflammatory response to biomaterials. *J Thromb Haemost* 2004; **2**: 1798–805.